Materials Science in Semiconductor Processing 17 (2014) 81–86

Contents lists available at ScienceDirect

Materials Science in Semiconductor Processing

journal homepage: www.elsevier.com/locate/mssp

Effect of alkali treatment on the spectral response of silicon-nanowire solar cells

Yurong Jiang*, Ruiping Qin, Meng Li, Guangna Wang, Heng Ma, Fanggao Chang*

College of Physics & Electrics Engineering, Henan Normal University, Henan Key Laboratory of Photovoltaic Materials, Xinxiang 453007, PR China

ARTICLE INFO

Available online 23 September 2013

Keywords:
Silicon nanowires
Metal-assisted etching
Alkali treatment
Spectral response

ABSTRACT

The effect of alkali treatment of Si nanowires (SiNWs) on the spectral response of solar cells was investigated using monochromatic incident photon-to-electron conversion efficiency spectroscopy. SiNWs were prepared on a substrate by metal-assisted etching and were then treated with NaOH/isopropanol. The results show that alkali treatment of SiNWs for 30 s obviously improved the cell conversion efficiency. This was attributed to enhancement of the red light response and a decrease in surface reflectivity from 6% to ~2%. However, SiNW alkali treatment led to poor blue light response, which is a major limiting factor for efficient SiNW solar cells. To improve the photovoltaic properties of SiNW cells, a near-complete response over the whole solar spectrum is essential.

1. Introduction

Silicon nanowires (SiNWs) are attractive because of their unique electrical and optical properties compared to bulk silicon, so they are potential candidates for cost-effective, third-generation, high-efficiency solar cells [1–4]. In particular, SiNWs vertically aligned to the substrate demonstrate excellent broadband antireflection owing to strong light trapping by multiple scattering of incident light [5–10] and the optical antenna effect [11]. As a simple and low-cost process for silicon photovoltaic applications, metal-assisted chemical etching for SiNW fabrication has attracted much attention [10,12–15]. SiNWs can form in various crystallographic orientations on silicon surfaces [16–19].

Surface pretreatment of silicon wafers causes an increase in SiNW density and improves the uniformity of SiNW arrays [20]. KOH dipping is a simple and cost-effective process that can be used to separate NWs from bundles by tapering them; this improve the antireflection and photovoltaic characteristics of NWs [21]. Surface treatment plays an important role in SiNW morphology and in suppressing reflection. A micrometer-scale texture forms a thin reflecting film and enhances photon absorption, mainly via a geometric optical effect. However, there has been no investigation into the effect of alkali treatment of SiNWs as an absorber layer on planar components using monochromatic incident photon-to-electron conversion efficiency (IPCE) spectroscopy to date.

We investigated the effect of alkali treatment on the spectral response of SiNW cells using IPCE spectroscopy. We found that 30 s treatment improved the light response of SiNW solar cells over the range 450–1100 nm. However, alkali-treated SiNW solar cells showed a poor blue light response, which is a major limiting factor for efficient SiNW cells.

2. Experimental

Polished p-type Si (100) wafers (0.1–1 Ω/cm, 5 cm in diameter) were ultrasonically cleaned in acetone and in ethanol at room temperature for 10 min to remove organic

* Corresponding authors.
E-mail addresses: jiangyurong@whut.edu.cn (Y. Jiang), chfg@henannu.edu.cn (F. Chang).

1369-8001/$ - see front matter © 2013 Elsevier Ltd. All rights reserved.
http://dx.doi.org/10.1016/j.mssp.2013.08.011

contaminants. The clean wafers were immediately immersed in an aqueous solution of 5 M HF and 0.02 M $AgNO_3$ for 30 min for growth of vertically aligned SiNWs in a simple Teflon vessel. After etching, the samples were wrapped with a thick dendritic Ag structure [22]. Silver nanoparticles were easily removed after electroless etching by dipping the samples in nitric acid (68 wt%) for 120 min. The samples were then rinsed with deionized water, dipped in 10 wt% HF solution to remove native oxide, rinsed with deionized water again, and dipped in a solution of 30 wt% NaOH and 10 wt% isopropyl alcohol (IPA) at 25 °C. IPA increases the wettability of crystalline silicon surfaces in alkaline etching solutions [23].

A control sample was prepared by dipping a Si (100) wafer into a solution of 30 wt% NaOH and 10 wt% IPA for 30 min at 80 °C; this led to a silicon etch depth of approximately 5–10 μm.

Solar cells were fabricated using SiNWs according to the following steps. (1) The substrate was heated in a 3:1 mixture of 97% H_2SO_4 and 30% H_2O_2 for 10 min to remove organic residues and heavy metals. (2) Cleaned wafers were rinsed thoroughly with deionized water and then 1% HF solution to remove native oxide. (3) Phosphorus oxychloride was spin-coated onto SiNWs on a wafer. (4) Phosphorus-coated wafers were heated in a tube furnace at 930 °C for 10 min. This led to phosphorus ion doping of the NW wafer surface via thermal diffusion to form a bulk p–n junction on the samples. SiNWs ought to be n-type after phosphorus diffusion [9].

The depth of the diffusion layer on the underlying wafer was estimated as ~300–500 nm according to a chemical coloration method. The sheet resistance was controlled at approximately 46.3 Ω/□ as measured using a four-point probe. To assess the effect of light absorption by SiNWs on the photovoltaic response, we printed silver paste as the front and rear electrodes of the p–n junction over an area of 0.5 cm^2.

Fig. 1 shows a schematic of the fabrication process for SiNW solar cells. The as-synthesized SiNWs were characterized using a scanning electron microscope (SEM; Jeol 6301F). SiNWs-based solar cells with an area of 1×1 cm^2 were cut out. Reflectivity and transmittance measurements were carried out on a UV-3600 spectrophotometer equipped with an integrating sphere and a photomultiplier tube and PbS for detection over the wavelength range 300–1300 nm. The light source was a halogen lamp. The internal quantum efficiency (IQE) of the cells was characterized using a Newport 1000-W halogen lamp and a grating monochromator (Acton Spectra Pro 2300i) with an SR540 optical chopper and a lock-in amplifier (SR-830) to avoid electrical and optical interference. A calibrated Newport 818-UV sensor was used to measure the absolute IQE of the solar cells under AM 1.5 illumination.

3. Results and discussion

The cross-sectional SEM image in Fig. 2a shows NWs of ~8 μm in length with excellent vertical alignment to the substrate. The tilted SEM image in Fig. 2b demonstrates the overall morphology of the electroless etched SiNWs and reveals a bunched morphology between the top ends of the as-etched NWs. NW bundles were observed due to agglomeration at their tops ends [21]. This agglomeration can be attributed to van der Waals forces between the NWs. The tilted SEM images in Fig. 2c,d illustrate the effect of the NaOH/IPA etching time on the NW array morphology. Agglomerated top ends of the NWs were easily separated by even short (30 s) treatment with NaOH/IPA (Fig. 2c).

The wet etching rate of single-crystal Si depends heavily on the bond strength of surface atoms [24]. Top corner edges in a square microstructure have weak bond strength owing to the drastic transition in surface atom density at the corners. This results in a faster etching rate at the corners than over flat regions, so convex undercutting is clearly visible and a sharp tip and tapered shape form on the top [21].

Therefore, we used an anisotropic etching process after metal-assisted etching to decrease van der Waals forces between NWs and separate NW bundles. When the etching time was increased to 60 s, the NWs almost disappeared (Fig. 2d), exposing the rugged surface morphology. It is clear from the SEM images that alkali treatment significantly changed the NW morphology. Etching led to separation of tapered single NWs, in accordance with previous research [21].

The morphology of the textured wafer used as a control shows uneven pyramid structures on the sample surface (Fig. 2e). This confirms that alkali etching of Si (100) leads to a textured surface because of the anisotropic etching behavior of crystalline Si [25].

After removal of the silver layer, etched silicon wafers were dark black in appearance, which is indicative of low surface reflectivity. Photons reflected from a photovoltaic cell surface are neither absorbed nor converted to electricity. This motivated us to investigate the reflectivity of our samples. Total reflectance spectra were measured on a UV-3600 spectrophotometer (Fig. 3a). Compared to SiNWs and the random pyramid structure formed on the textured

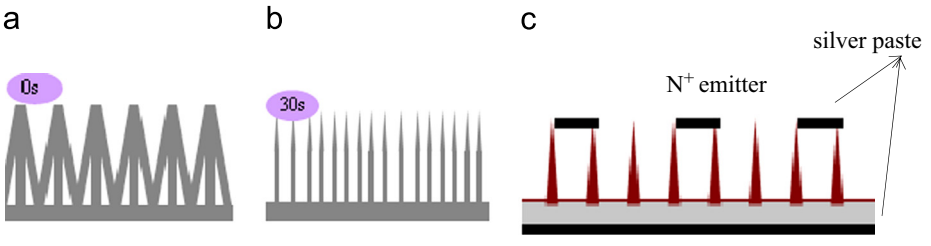

Fig. 1. Schematic illustration of the fabrication process for SiNW-array solar cells. (a) Formation of bundled SiNW arrays on the wafer. (b) Alkali treatment of SiNWs for 30 s. (c) Formation of an n-type emitter by phosphorus diffusion and electrode on the rear and front surfaces.

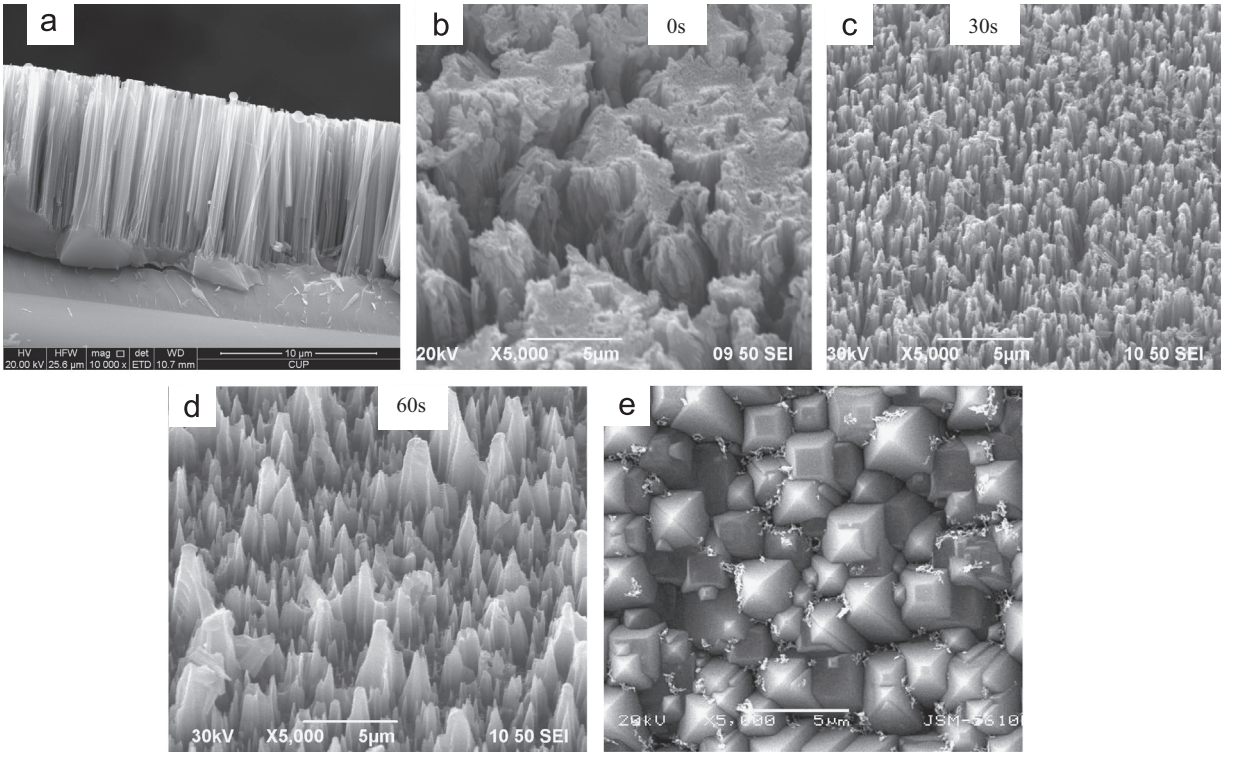

Fig. 2. SEM images showing the SiNW array and textured surface. (a) Cross-sectional SEM image showing the morphology after metal-assisted electroless etching. SEM images tilted by 30° for (b) untreated sample, (c) sample treated in NaOH/IPA for 30 s, and (d) sample treated in NaOH/IPA for 60 s. (e) SEM image of the NaOH/IPA-textured Si surface.

control sample, the reflectance of NWs subjected to alkali treatment for 30 s greatly decreased to an average of ~2% over the whole wavelength range. Thus, 30-s alkali treatment of SiNWs improved their antireflection property in the wavelength range 300–1300 nm. However, for the longer alkali treatment time of 60 s, the SiNW reflectance was higher, at >4%. The results demonstrate that alkali treatment of SiNWs for 30 s is beneficial for solar energy trapping. The ultrahigh surface area of tapered SiNWs causes multiple scattering of sunlight, which enhances light trapping and leads to much lower reflectance [6].

We also investigated the effect of alkali treatment on light absorption. Total absorption can be expressed as $A = 100–R–T$, where R is reflectance and T is transmittance. The total light absorption for NWs subjected to 30-s alkali treatment was >97% (Fig. 3b). The spectra confirm that 30-s alkali treatment improved the absorption of NWs over the wavelength range 300–1300 nm.

Two processes are required for a working solar cell: light absorption and photogenerated carrier collection. To verify the effect of alkali treatment on photogenerated carrier collection, we measured IQE for solar cells prepared using four typical samples: NaOH/IPA-textured Si wafers, SiNWs, and SiNWs subjected to alkali treatment for 30 s and 60 s, respectively. The IQE (generated and effectively utilized electron–hole pairs) of a solar cell is related to the external quantum efficiency (EQE) according to IQE = EQE/(1–R–T). IQE curves for the four samples are shown in Fig. 4. The highest IQE was observed for the solar cell prepared with SiNWs subjected to 30-s alkali treatment (~33.75% at 520 nm). Lower IQE was observed when the alkali treatment time was increased to 60 s because light absorption decreases with the SiNW area density. The results suggest that the cell based on SiNWs subjected to 30-s alkali treatment has high collection efficiency for minority carriers. The maximum IQE was 27.18% at 460 nm for the cell prepared with a textured control wafer and 30.18% at 520 nm for the cell prepared with untreated SiNWs, which represents a red shift of 60 nm compared to the textured control.

Although the cell prepared with SiNWs subjected to 30-s alkali treatment showed an improvement in photoelectric response at long wavelength (Table 1), its blue light response was poor, which implies that not all the photogenerated carriers were collected. Surface recombination losses might limit the carrier collection efficiency and reduce the blue light response [26]. In addition, the red shift of the maximum IQE indicates that a charge carrier loss mechanism, such as recombination on the front surface, in the emitter layer or in the p–n junction, limits the blue IQE. Considering the conflicting factors of increased surface recombination and light-trapping effectiveness, surface passivation may help to optimize the overall performance of SiNW solar cells. Surface passivation (such as deposition of Al_2O_3 and amorphous silicon on NWs) could reduce surface recombination and improve the photosensitivity of nano-Si for solar cells [27,28] and thus increase the final conversion efficiency.

Alkali treatment should significantly decrease typical geometric factors for SiNWs, including the wire diameter

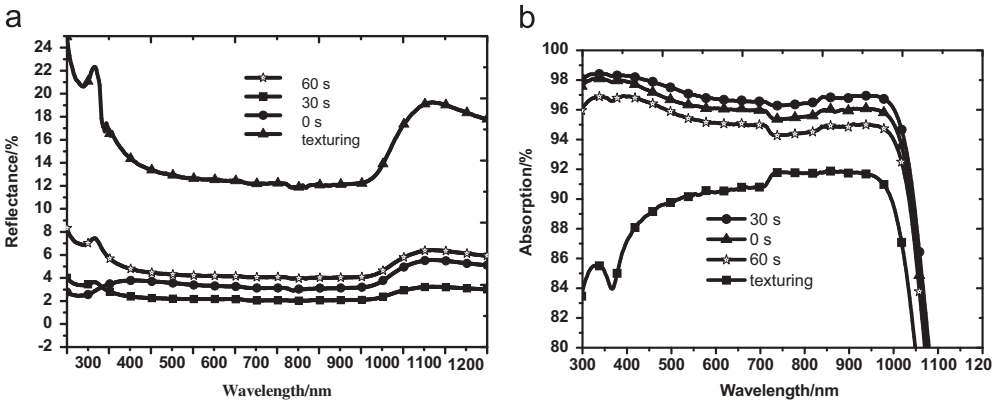

Fig. 3. (a) Optical reflectance and (b) absorption spectra of the textured wafer, SiNWs, and samples treated with NaOH/IPA.

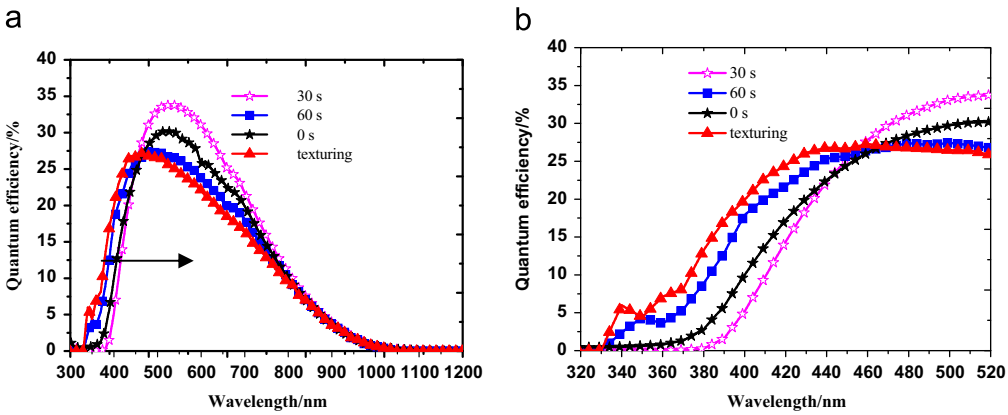

Fig. 4. (a) Internal quantum efficiency spectra for SiNW array solar cells after NaOH/IPA treatment for different etching times. (b) Spectral response in the short wavelength range.

Table 1
Greatest quantum efficiency and corresponding wavelength.

	Alkali treatment			Textured
	0 s	30 s	60 s	surface
Quantum efficiency (%)	30.18	33.75	27.42	27.18
Corresponding wavelength (nm)	520	520	500	460

and length, and should thus affect the optical properties. Tapering increases the surface to volume ratio (relative to SiNWs with the same volume) and the variation in diameter along the wire alters quantum confinement in a manner analogous to wires with different surface reconstructions [29,30]. Tapered NWs also provide an opportunity to use new charge separation mechanisms [31]. The results are consistent with previous research indicating that differences in size and cross-sectional morphology affect the optical properties [32–34].

The current density–voltage (J–V) characteristics of SiNW cells were measured. The dark J–V curve shows typical rectifying behavior and confirms the formation of a p–n junction (Fig. 5a). The SiNW solar cell performance under AM 1.5G illumination is shown in Fig. 5b. and is summarized in Table 2. The results demonstrate that compared to untreated SiNWs, alkali treatment for 30 s increased the short-circuit current density (J_{sc}) from 10.65 to 12.51 mA/cm^2 (19.7% enhancement) and the conversion efficiency from 1.9% to 2.5%. The highest open-circuit voltage (V_{oc}) was also obtained for the cell with SiNWs subjected to alkali treatment for 30 s. In general, alkali treatment of SiNWs for 30 s led to an overall improvement in cell performance. This is largely due to higher J_{sc}, which can be attributed to increases in the light absorption and spectral response at long wavelength.

Although alkali treatment for 30 s decreased the series resistance from 626.7 Ω to 516.3 Ω, the conformal coating of Ag paste over tapered Si leads to large serial resistance of 516.3 Ω cm^2, which causes high contact resistance between the Si and the electrode and can negatively affect device performance. Various methods can be used to make an ohmic contact, among which formation of a highly doped Si layer is commonly used for high-efficiency Si solar cells. The highly doped layer not only decreases the contact resistance but also forms a built-in electric field on the back side that deflects minority carriers and reduces the recombination rate at the back surface, which can significantly increase the saturation current density and improve V_{oc} [35].

Therefore, optimized electrode design and processing are required to further improve the performance of SiNW array-based solar cell. Moreover, the IQE and cell performance

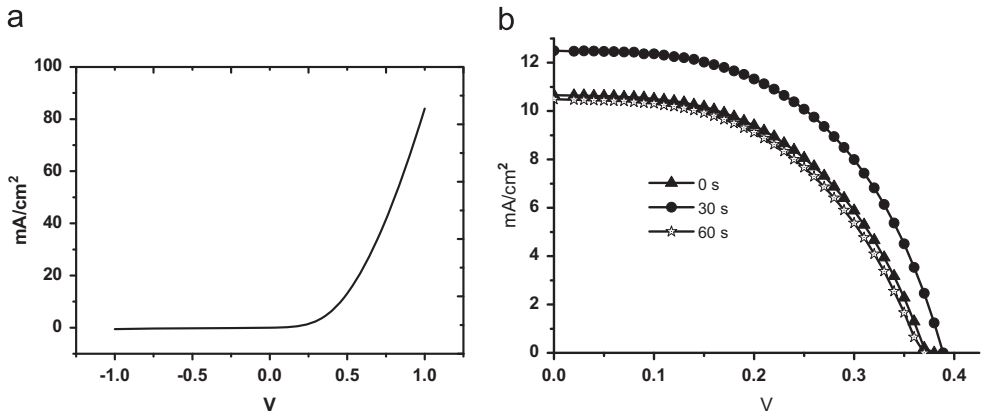

Fig. 5. Current density–voltage characteristics of the nanowire device (a) in the dark and (b) under solar illumination of 100 mW cm^{-2} AM 1.5G.

Table 2
Photovoltaic performance of SiNW solar cells.

Alkali treatment (s)	V_{oc} (V)	J_{sc} (mA/cm^2)	FF (%)	Effective area (cm^2)	Serial resistance (Ω)	Conversion efficiency (%)
60	0.368	10.45	50.6	0.5	597.6	1.9
30	0.389	12.51	52.1	0.5	516.3	2.53
0	0.372	10.65	51.8	0.5	626.7	2.1

might be further improved by adapted phosphorous diffusion, SiNWs surface modification might reduce the surface recombination, so as to realize near-complete response throughout the whole solar spectrum.

4. Conclusion

The effect of alkali treatment on the spectral response of SiNW cells was investigated using IPCE spectroscopy. The results show that alkali treatment modifies the morphology and spectral response of SiNWs. Although 30 s alkali treatment led to very low surface reflectance and improved the conversion efficiency of SiNW cells, the blue light response was poor. Recombination loss might play an important role in the low blue light response. Surface passivation might reduce surface recombination and improve the photosensitivity of nano-Si solar cells. This approach could increase the final conversion efficiency to satisfy high-efficiency standards.

Acknowledgments

This work was supported by Chinese Natural Science Foundation (No. 11074066) and Henan Provincial Basic and Frontier project (No. 132300410248).

References

[1] Y.M. Song, J.S. Yu, Y.T. Lee, Opt. Lett. 35 (2010) 276–278.
[2] C.K. Chan, H.L. Peng, G. Liu, K. Mcllwrath, X.F. Zhang, R.A. Huggins, Y. Cui, Nat. Nanotechnol. 3 (2008) 31–35.
[3] S.W. Boettcher, J.M. Spurgeon, M.C. Putnam, E.L. Warren, D.B. Turner-Evans, M.D. Kelzenberg, J. Rmaiolo, H.A. Atwater, N.S. Lewis, Science 327 (2010) 185–187.
[4] E.C. Garnett, P. Yang, J. Am. Chem. Soc. 130 (2008) 9224–9225.
[5] C. Lin, M.L. Povinelli, Opt. Express 17 (2009) 19371–19381.
[6] V.V. Iyengar, B.K. Nayak, M.C. Gupta, Sol. Energy Mater. Sol. Cells 94 (2010) 2251–2257.
[7] H.M. Branz, V.E. Yost, S. Ward, K.M. Jones, B. To, P. Stradins, Appl. Phys. Lett. 94 (2009) 231121.
[8] M. Ben Rabha, A. Hajjaji, B. Bessais, Sol. Energy 86 (2012) 1411–1415.
[9] D. Kumar, S.K. Srivastava, P.K. Singh, M. Husain, V. Kumar, Sol. Energy Mater. Sol. Cells 95 (2011) 215–218.
[10] S.K. Srivastava, D. Kumar, Vandana, M. Sharma, R. Kumar, P.K. Singh, Sol. Energy Mater. Sol. Cells 100 (2012) 33–38.
[11] E. Garnett, P. Yang, Nano Lett. 10 (2010) 1082–1087.
[12] K. Peng, A. Lu, R. Zhang, S.T. Lee, Adv. Funct. Mater. 18 (2008) 3026–3035.
[13] M.L. Zhang, K.Q. Peng, X. Fan, J.S. Jie, R.Q. Zhang, S.T. Lee, N.B. Wong, J. Phys. Chem C112 (2008) 4444–4450.
[14] K. Peng, X. Wang, S.T. Lee, Appl. Phys. Lett. 92 (2008) 163103.
[15] Y. Wang, Y.P. Liu, H.L. Liang, Z.X. Mei., X.L. Du, Phys. Chem. Chem. Phys. 15 (2013) 2345–2350.
[16] C.Y. Chen, C.S. Wu, C.J. Chou, T.J. Yen, Adv. Mater. 20 (2008) 3811–3815.
[17] K. Peng, M. Zhang, A. Lu, N.B. Wong, R. Zhang, S.T. Lee, Appl. Phys. Lett. 90 (2007) 163123.
[18] N. Geyer, Z. Huang, B. Fuhrmann, S. Grimm, M. Reiche, T. Nguyen-Duc, J. de Boor, H.S. Leipner, P. Werner, U. Gosele, Nano Lett. 9 (2009) 3106–3110.
[19] Z. Huang, T. Shimizu, S. Senz, Z. Zhang, X. Zhang, W. Lee, N. Geyer, U. Gösele, Nano Lett. 9 (2009) 2519–2525.
[20] C. Shiu, S.B. Lin, S.C. Hung, C.F. Lin, Appl. Surf. Sci. 257 (2011) 1829–1834.
[21] Y. Jung, Z. Guo, S.W. Jee, H.D. Um, K.T. Lin, J.-H. Lee, Opt. Express 18 (Suppl. 3) (2010) A286–A292.
[22] K.Q. Peng, Z.P. Huang, J. Zhu, Adv. Mater. 16 (2004) 73–76.
[23] Y.Y. Zhang, J. Zhang, G. Luo, X. Zhou, G.Y. Xie, T. Zhu, Z.F. Liu, Nanotechnology 16 (2005) 422–428.
[24] C.R. Tellier, A.R. Charbonnieras, Sensors Actuators A 105 (2003) 62–75.
[25] K. Ali, S.A. Khan, M.Z. Mat Jafri, Superlattices Microstruct 52 (2012) 782–792.
[26] F. Toor, H.M. Branz, M.R. Page, K.M. Jones, H.-C. Yuan, Appl. Phys. Lett. 99 (2011) 103501.

[27] K. Takei, J.H. Meza, A. Javey, K.B. Crozier, Nano Lett. 11 (2011) 2527–2532.
[28] J.H. Oh, H.-C. Yuan, H.M. Branz, Nat. Nanotechnol. 7 (2012) 743–748.
[29] R. Rurali, A. Poissier, N. Lorente, Phys. Rev. B 74 (2006) 165324.
[30] T. Vo, A.J. Williamson, G. Galli, Phys. Rev. B 74 (2006) 045116.
[31] Z. Wu, J.B. Neaton, J.C. Grossman, Phys. Rev. Lett. 100 (2008) 246804.
[32] L. Hu, G. Chen, Nano Lett. 7 (2007) 3249–3252.
[33] J. Li, H. Yu, S.M. Wong, G. Zhang, X. Sun, P.G. Lo, D.-L. Kwong, Appl. Phys. Lett. 95 (2009) 033102.
[34] S.-K. Kim, R.W. Day, J.F. Cahoon, T.J. Kempa, K.-D. Song, H.-G. Park, C. M. Lieber, Nano Lett. 12 (2012) 4971–4976.
[35] S.M. Jeong, E.C. Garnett, S. Wang, Z.F. Yu, S.H. Fan, M.L. Brongersma, M.D. McGehee, Y. Cui, Nano Lett. 12 (2012) 2971–2976.